Effect of tin doping on oxygen- and carbon-related defects in Czochralski silicon

Journal Item

Effect of tin doping on oxygen- and carbon-related defects in Czochralski silicon

A. Chroneos,[1,a)] C. A. Londos,[2,a)] and E. N. Sgourou[2,a)]
[1]*Department of Materials, Imperial College London, London SW7 2AZ, United Kingdom*
[2]*University of Athens, Solid State Physics Section, Panepistimiopolis Zografos, Athens 157 84, Greece*

(Received 11 August 2011; accepted 29 September 2011; published online 3 November 2011)

Experimental and theoretical techniques are used to investigate the impact of tin doping on the formation and the thermal stability of oxygen- and carbon-related defects in electron-irradiated Czochralski silicon. The results verify previous reports that Sn doping reduces the formation of the *V*O defect and suppresses its conversion to the VO_2 defect. Within experimental accuracy, a small delay in the growth of the VO_2 defect is observed. Regarding carbon-related defects, it is determined that Sn doping leads to a reduction in the formation of the C_iO_i, C_iC_s, and $C_iO_i(Si_I)$ defects although an increase in their thermal stability is observed. The impact of strain induced in the lattice by the larger tin substitutional atoms, as well as their association with intrinsic defects and carbon impurities, can be considered as an explanation to account for the above observations. The density functional theory calculations are used to study the interaction of tin with lattice vacancies and oxygen- and carbon-related clusters. Both experimental and theoretical results demonstrate that tin co-doping is an efficient defect engineering strategy to suppress detrimental effects because of the presence of oxygen- and carbon-related defect clusters in devices. © *2011 American Institute of Physics*. [doi:10.1063/1.3658261]

I. INTRODUCTION

Czochralski silicon (Cz-Si) is one of the most important and widely used materials in the semiconductor industry. Applications of Si in certain electronic and optical devices require the introduction of impurities to improve the material properties. In this respect, doping of Si with group-IV isovalent impurities has attracted strong interest in the last 20 years.[1]

Isovalent impurities in Si [carbon (C), germanium (Ge), tin (Sn), and lead (Pb)], introduced at substitutional sites do not affect its electrical properties.[1] Among them, Ge, Sn, and Pb have a larger covalent radius ($r_{Ge} = 1.22$ Å, $r_{Sn} = 1.41$, and Å, $r_{Pb} = 1.44$ Å) than that of Si ($r_{Si} = 1.17$ Å), leading to compressive stresses in the Si lattice. Conversely, C is the lightest and has a smaller covalent radius ($r_c = 0.77$ Å) than Si, leading to tensile stresses as a substitutional impurity. Thus, isovalent impurities, being sources of internal stresses, may affect the various impurity defects and intrinsic point defect interactions.

In this study, we focus on C and Sn isovalent impurities in Cz-Si. Carbon is, other than oxygen, the most common impurity in Si and is introduced during crystal growth. Its influence on the Si properties and behavior is the subject of numerous investigations.[2] Sn, on the other hand, is purposely introduced in the Si lattice for certain technological applications, mainly in relation with the compensation of stresses in the lattice and its ability to capture vacancies (*V*).[1]

The compressive strains introduced by Sn are relieved by the capture of vacancies. Previous studies determined that the generation rate of vacancy-related defects such as *V*O (also known as the A-center) and divacancy (V_2), is substantially reduced in Si at the expense of the formation of Sn*V* pairs.[3–6] Conversely, the generation rate of interstitial-related defects seems insensitive to the Sn content in the lattice.[5,6] Thus, Sn can be used to characterize whether an unknown defect is vacancy or interstitial related. Using the same train of thought, C could have a similar role. The tensile strains, introduced by the carbon substitutional (C_s) in the lattice, are relieved by the capture of self-interstitials (Si_I). In this process, C_s is converted to interstitial carbon (C_i), which readily reacts with C_s and O_i defects to form the C_iC_s and the C_iO_i pairs, the main C-related defects in Si.[2] The ability of Sn and C to capture vacancies and self-interstitials, respectively, has led to suggestions of using Sn and C co-doped Si material to investigate and improve the radiation hardness of related devices.[5,7] Notably, co-doping Si with C and Sn has been determined to be an effective way to enhance the solubility of the two impurities because of the mutual compensation of each other's stresses in the lattice.[8] Apparently, the changes in the concentrations of intrinsic defects, as a result of the Sn and C presence, are expected to affect significantly the formation, properties, and, generally, the behavior of radiation-induced defects in Si.

The most studied defect in Sn-doped Si is the Sn*V* pair. Electron paramagnetic resonance (EPR) measurements have indicated that in this structure the Sn atom is located halfway between two semi-vacancies on adjacent lattice sites.[3,9] This model was verified by density-functional-theory (DFT) calculations.[10] Additional information was provided by deep-level transient spectroscopy (DLTS), positron annihilation spectroscopy (PAS), and Mössbauer spectroscopy measurements in conjunction with electronic structure calculations.[11]

[a)]Authors to whom correspondence should be addressed. Electronic addresses: alexander.chroneos@imperial.ac.uk, hlontos@phys.uoa.gr, and esgourou@phys.uoa.gr.

The *V*O pair has two well-known local vibrational mode (LVM) bands at about 830 and 890 cm^{-1}, relating to its neutral and negative charge state, respectively, and originating from the vibrations of the oxygen impurity in the *V*O structure.[12,13] However, no LVM bands have been reported so far for the Sn*V* defect. In infrared (IR) studies the presence of the Sn*V* pair is monitored in the spectra by the increase of the *V*O and V_2 corresponding bands above ~170 °C, because of the dissociation of the Sn*V* pairs.[4–6] At those temperatures, the release of vacancies leads to the subsequent formation of vacancy-related defects, mainly *V*O and V_2. Furthermore, at about 300 °C, *V*O pairs begin to migrate until they are trapped by oxygen atoms and transformed to VO_2 clusters.[14,15]

Additionally, experimental and theoretical works on the formation of Sn_nV_m, have verified the existence of SnV_2 and Sn_2V_2 complexes in Si, although no IR signals have been reported. Conversely, an IR band at 812 cm^{-1} (at 10 K) related to the Sn*V*O structure appears in the spectra.[16–18]

As mentioned, the two main C-related defects are the C_iO_i and C_iC_s pairs. Both pairs are electrically and optically active and have been studied intensively by numerous experimental techniques.[2,19–25] C_iO_i gives rise to a number of IR bands, the most intense being that at 862 cm^{-1}.[2,24] It anneals out from the spectra at about 300 °C. C_iC_s pairs give rise to a number of weak bands detected at cryogenic temperatures. One of them at about 544 cm^{-1} is observed also at room temperature.[2,25,26] Recent investigations have determined the 544 cm^{-1} band to be a contribution of two bands from the C_iO_i and C_iC_s pairs.[27] The C_iC_s pair anneals out at about 250 °C.[2,26] On heavier doses, the C_i, C_iO_i and C_iC_s pairs act as nucleation sites for self-interstitials leading to the formation of $C_i(Si_I)$, $C_iO_i(Si_I)$, and $C_iC_s(Si_I)$ complexes.[2,28]

It has been reported that the annealing temperature of *V*O defect decreases with the increase of Ge content of Ge-doped Cz-Si, although the annealing temperatures of the C_iO_i and C_iC_s pairs are practically unaffected.[29] In previous studies we have investigated the effect of Ge doping on the behavior of radiation induced defects in Si.[29–33] In the present work, we extended these studies by investigating the effect of Sn doping on the oxygen-related (*V*O, VO_2) and carbon-related [C_iO_i, C_iC_s and $C_iO_i(Si_I)$] defects in Cz-Si. To complement the experimental results we used DFT to investigate the interaction of Sn with important clusters and defects.

II. METHODOLOGY

A. Experimental methodology

We used two groups of 2-mm-thick Sn-doped Cz-Si samples, one with low Sn concentration $[Sn] = 0.3 \times 10^{18}$ cm^{-3}, labeled Sn_L, and another one with relatively high Sn concentration $[Sn] = 9 \times 10^{18}$ cm^{-3}, labeled Sn_H. The Sn concentrations of the samples were measured by secondary ion mass spectrometry (SIMS) and the values were given by the supplier's certificate. The samples contained oxygen and carbon. The oxygen concentration was calculated from its 1106-cm^{-1} band using a calibration coefficient of 3.14×10^{17} cm^{-2}.[34] The carbon concentration was calculated from its 606-cm^{-1} band from using a calibration coefficient of 1×10^{17} cm^{-2}.[35]

The samples were irradiated with 2-MeV electrons at ~80 °C, with a fluence of 1×10^{18} cm^{-2}. Their Sn, O, and C content, as well as other details, are given in Table I. After the irradiation, the samples were subjected to 20-min isochronal anneals, at selective temperatures up to 600 °C. After each annealing step, the IR measurements were carried out at room temperature using a Fourier transform IR (FTIR) spectrometer operating at a resolution of 1 cm^{-1}. The two-phonon intrinsic absorption was always removed by subtracting the spectrum of a float zone (Fz-Si) sample of equal thickness.

B. Theoretical methodology

To study the interactions between Sn and O or C related defects in Si, we employed the DFT code CASTEP using the Perdew-Burke-Ernzerhof (PBE) generalized gradient approximation (GGA) functional and ultrasoft pseudopotentials.[36–38] The 64-atom Si supercell was repeated in space with the application of periodic boundary conditions. The plane wave basis energy cutoff was 350 eV and the Monkhorst-Pack $(2 \times 2 \times 2)$ *k*-point sampling was used.[39] Here the unit-cell parameters and atomic coordinates were relaxed using energy minimization with the criterion that the largest forces were less than 0.05 eV/Å and a total energy convergence tolerance not exceeding 10^{-5} eV/atom. These parameters adequately describe the structure and defect chemistry of Si and related materials.[40–43] For Sn-doped Si there are a number of recent DFT studies using the present methodology.[44,45]

III. RESULTS AND DISCUSSION

Figures 1(a) and 1(b) show the IR spectra of the Sn_L and Sn_H samples recorded just after irradiation, as well as at the temperatures of 250 and 400 °C in the course of the 20-min isochronal anneals. After irradiation, the well-known bands of *V*O (830 cm^{-1}), C_iO_i (862 cm^{-1}), C_iC_s/C_iO_i (546 cm^{-1}), and $C_iO_i(Si_I)$ [936 (1020) cm^{-1}] are observed in the spectra. At 250 °C, the $C_iO_i(Si_I)$ are not present, indicating that the defect has vanished. Two bands at 947 and 967 cm^{-1} have appeared. Their origin has not been definitely established but recent theoretical calculations relate them to higher-order members of the $C_iO_i(Si_I)_n$ $(n > 1)$ family.[46] At 400 °C, the *V*O band has

TABLE I. Details of the samples

Sample name	[Sn] 10^{18} cm^{-3}	$[O_i]_o$ 10^{17} cm^{-3}	$[C_s]_o$ 10^{17} cm^{-3}	a_{VO} cm^{-1}	a_{VO2} cm^{-1}	a_{VO2}/a_{VO}	a_{CiOi} cm^{-1}	$a_{CiCs/CiOi}$ cm^{-1}	$a_{CiOi(SiI)}$ cm^{-1}
Sn_L	0.3	9.6	4.7	1.2	0.4	0.33	0.63	0.2	0.12
Sn_H	9	9.2	2	0.8	0.12	0.15	0.49	0.18	0.05

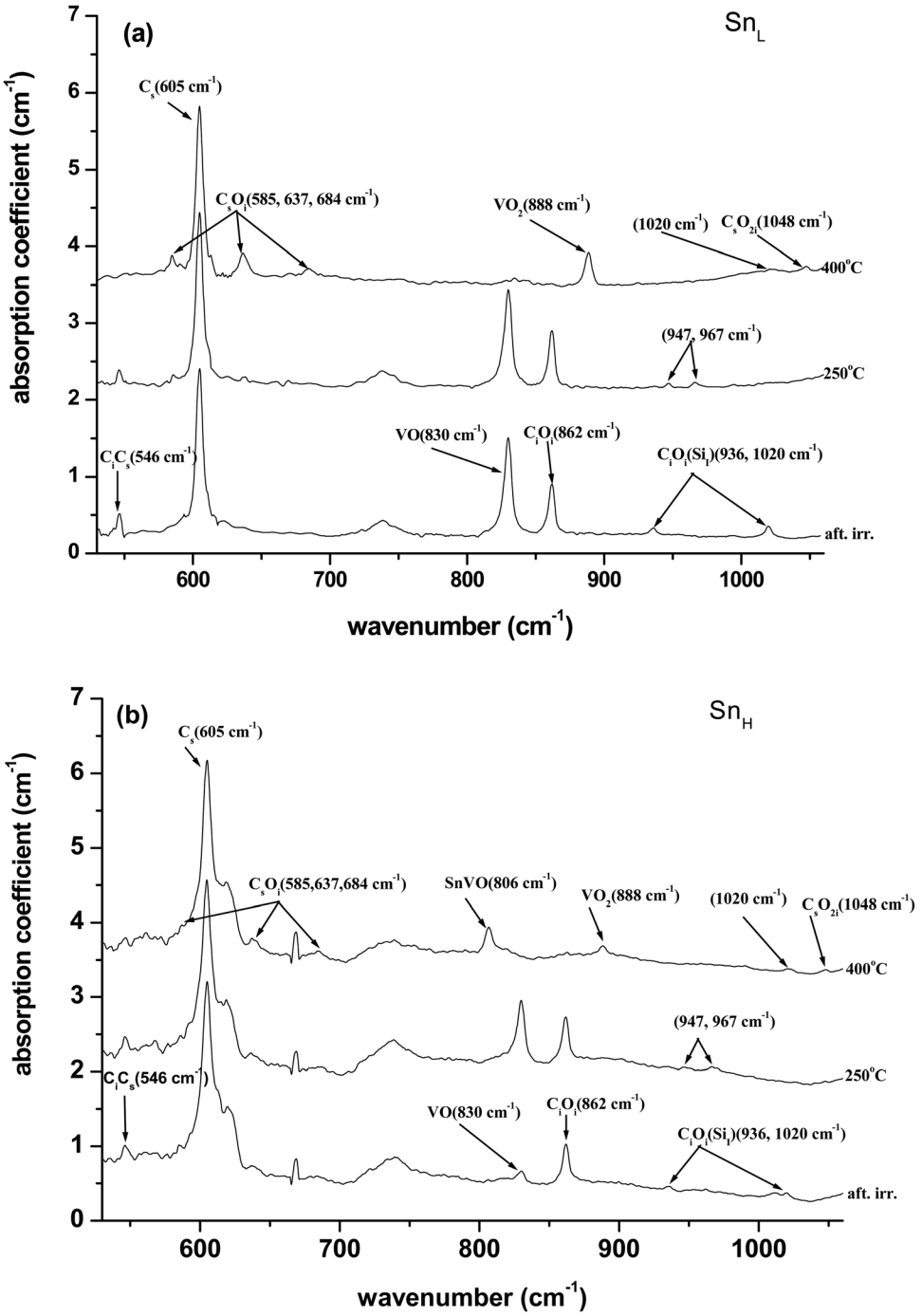

FIG. 1. Segments of IR absorption spectra of the Sn_L (a), and Sn_H (b) samples after irradiation and at 250 and 400 °C, in the course of the 20-min isochronal anneals.

been replaced by a band at 888 cm^{-1} attributed to the VO_2 defect ($VO + O_i \rightarrow VO_2$).[12,14,47] Also, a band at 806 cm^{-1}, attributed to the SnVO defect (Sn + VO → SnVO), is present in the spectra of the Sn_H sample.[18] We note that this band does not appear in the Sn_L sample. The disappearance upon annealing of the 862-cm^{-1} C_iO_i band from the spectra has been accompanied by a band at 1048 cm^{-1}, attributed to the C_sO_{2i} defect.[48] Also, bands at 585, 637, and 684 cm^{-1} could be clearly observed, at this temperature. Traces of these bands are detected even before irradiation. In the literature they have been labeled as X, Y, and Z bands, respectively, and were attributed to the C_sO_i defect.[2]

Figures 2(a) and 2(b) demonstrate the evolution with temperature of the VO and VO_2 bands for the Sn_L and Sn_H samples, respectively. Initially it is observed that the production of the VO pair is largely suppressed in the Sn_H sample in agreement with previous reports.[3–6] A number of the vacancies produced by irradiation, in particularly those escaped annihilations by self-interstitials, are captured by Sn impurities leading to the formation of the SnV pair. The interaction of Sn with a V to form a SnV pair has been previously studied using DFT in both the GGA and the local density approximation (LDA).[10,41] There is consensus in the literature that the split-vacancy configuration is more energetically favorable than the full-vacancy configuration in Si and isostructural semiconductors such as Ge.[10,41,49] Using the present GGA/DFT methodology (as described in Sec. IIB), the binding energy difference between the two

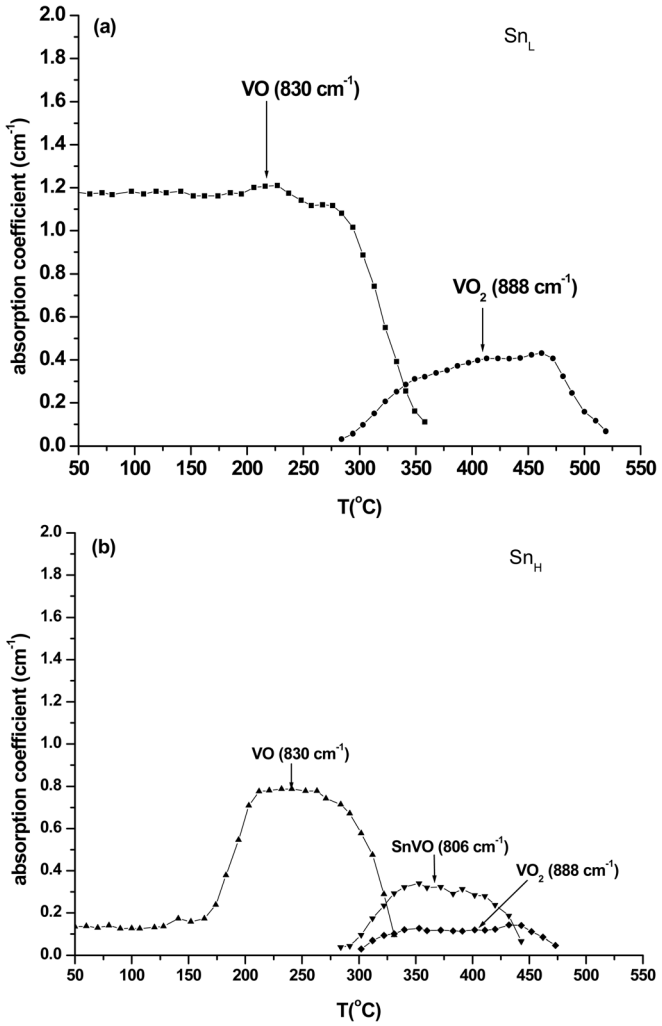

FIG. 2. The thermal evolution of the VO, VO_2, and SnVO defects for the Sn_L (a), and Sn_H (b) samples.

configurations is only 0.02 eV in Si. Larger Sn_mV_n clusters are also predicted to be bound as discussed in detail in previous work.[45]

Actually, Sn competes with O_i in capturing vacancies leading in a reduction of the VO formation. The SnV pair dissociates (Sn$V \rightarrow$ Sn $+ V$) at 170 °C. Because it is IR inactive, its presence in the material is verified by the corresponding increase of the VO and the V_2 centers.[4–6] This is reflected in the evolution curves of VO in the Sn_H sample [Fig. 2(b)], where above 170 °C we have a substantial increase in the concentration of VO defect. Notably, such an increase is not observed for the Sn_L sample indicating that for low Sn concentration below 10^{18} cm^{-3} the effect of Sn doping may be considered negligible. This is in agreement with previous reports.[50] The final VO concentration of the VO defect in the Sn_H sample is smaller than that in the Sn_L sample. Two possible reasons could account for this observation. First, the Sn_L sample contains a higher carbon concentration and it has been reported that VO formation is enhanced with the increase of carbon.[51] Second, at around 170 °C, where SnV begins to dissociate, self-interstitials may also be present. At around the same temperature, an EPR signal Si-P6 attributed to the di-interstitial defect begins to decay.[52] A possible release of self-interstitials would annihilate a fraction of the vacancies from the dissociation of the SnV defect, which is reflected in the spectra by the lower final concentration of the VO defect in the Sn_H sample. Additionally, the formation of SnV_2 defects indicates that some of the vacancies form other clusters apart from the VO defects.[16] Previous DFT investigations calculated that the SnV_2 clusters can be bound with up to -2.76 eV.[45] Therefore, when a migrating V_2 pair (binding energy $=-1.58$ eV, Ref. 45) encounters a Sn atom, it will strongly associate with it as the energy of the resultant cluster (i.e., SnV_2) will increase by -1.18 eV.

Another important observation is that the conversion of the VO to the VO_2 cluster is largely suppressed in the Sn_H sample. This is mostly because part of the VO defects are captured by Sn to form SnVO centers, consistently with previous reports.[53] From a DFT perspective, it was previously calculated that the interaction of Sn substitutionals with O_i is repulsive by 1.26 eV.[54] This is anticipated as the Sn atom is larger than the Si atom it substitutes and it therefore reduces the available space for the O_i. The pair interactions (i.e., SnV attracted by -1.30 eV and SnO_i repelled by 1.26 eV) influence the binding of A-centers in the presence of Sn and the configurations of the two possible nearest-neighbor clusters SnVO and SnOV (refer to Fig. 2 of Ref. 54). That is, the SnVO cluster is significantly more bound than the VO pair because of the beneficial interaction of the SnV (in SnVO, Sn is nearer to V).[54] Conversely, in the SnOV cluster, the repulsive interaction of SnO_i (in SnOV, Sn is nearer to O_i) results in a reduction of the binding energy as compared to VO.[54] Simply summarized, the Sn atom will increase the binding energy and trap a migrating VO pair only if it is in the side of the V. Thus, the DFT calculations support the experimental finding of the reduction of the VO_2 to VO ratio because of the formation of the SnVO. Moreover, they provide information on the favorable configuration of SnVO.

By inspection of the evolution curves of VO and VO_2 defects as they are depicted in Figs. 2(a) and 2(b), it is really difficult to draw any certain conclusions about the effect of Sn doping on the annealing temperature of VO defect. A comparison of the annealing curves of VO defects does not give clear evidence about certain differences in the temperature that characterize the onset of the decay of the 830-cm^{-1} band between the Sn_L and the Sn_H samples. It is worth noting that a small delay in the growth of the VO_2 defect is observed in the Sn_H sample. VO_2 seems to grow in the spectra at a slightly higher temperature, about 20 °C larger in the Sn_H sample than that of the Sn_L sample. Notably, a previous systematic study of the phenomenon in Ge-doped Si, using samples with Ge concentrations in the range 1×10^{17}–2×10^{20} cm^{-3} has shown that both the annealing temperature of VO and the growth temperature of VO_2 defect are decreased with the increase of the Ge content.[29] Those observations were discussed by taking into account the effect of elastic stress induced by Ge atoms in the Si lattice, which have an effect on the main reactions $VO + O_i \rightarrow VO_2$, $VO + Si_I \rightarrow O_i$ involved in the annealing of the VO defect and its conversion to the VO_2 defect. Actually, Ge has a larger covalent radius than that of Si. It introduces compressive strain in the lattice, which influences the onset of the

above reactions and the balance between them regarding the VO to VO_2 conversion. Because, however, Sn has an even larger covalent radius than that of Si, one would expect higher compressive strains in the lattice and, therefore, the above phenomena to appear more pronounced. Nevertheless, the impact of Sn doping show an opposite trend at least as far as the temperature of the growth of the VO_2 defect is concerned. The present results, however, are limited to two Sn concentrations, one lower than $10^{18}\,cm^{-3}$ and another one higher, around $10^{19}\,cm^{-3}$. The latter Sn concentration may be not high enough to verify clearly any differences between Sn and Ge impurities in Si on the properties of VO and VO_2 defects. However, from the differences between Sn and Ge, regarding their interactions with vacancies, self-interstitials, and oxygen impurities, one may expect some changes in the behavior of VO and VO_2 defects in Sn- and Ge-doped Si. For example, lattice vacancies are attracted more strongly by Sn (SnV binding energy $-1.30\,eV$) than Ge (GeV binding energy $-0.27\,eV$). Further studies are necessary to understand in detail the effect of Sn doping on the behavior of VO and VO_2 defect in Si doped with a wider range of Sn concentrations.

Figure 3 shows the evolution with temperature of the C_iO_i ($862\,cm^{-1}$) defects for the Sn_L and the Sn_H samples, respectively. Figures 4(a) and 4(b) show the evolution of the C_sO_i defects for the Sn_L and the Sn_H samples, respectively. Notice that in this temperature range, the $1048\,cm^{-1}$ band appears in the spectra and the intensities of the 585, 637, and $684\,cm^{-1}$ bands of the C_sO_i defect are enhanced.

At this point it is worth discussing the geometry and binding energy of the C_sO_i with respect to Sn, as it is an uncharted area. Using DFT, we calculate the binding energies of the C_sO_i pair [$-0.32\,eV$, Fig. 5(a)] and the SnC_sO_i cluster [$-0.62\,eV$, Fig. 5(b)].[54] For these clusters, not only all the nearest-neighbor but also the second-nearest-neighbor configurations were considered for all the constituent atoms of the cluster. The minimum energy configuration balances the repulsive interaction of the SnO_i (Sn and O_i at a distance

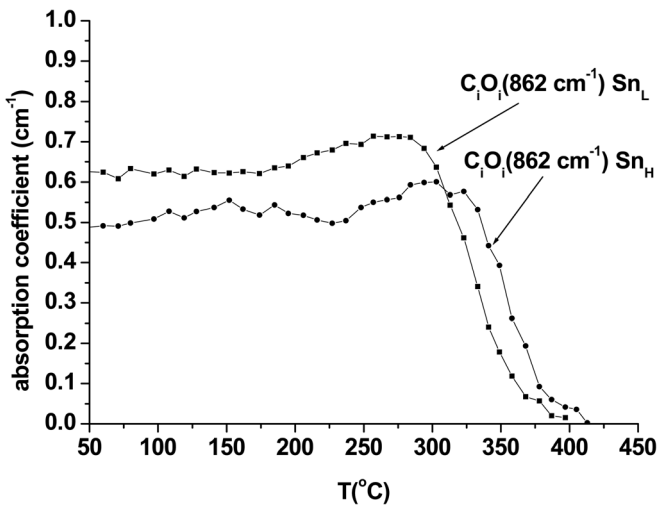

FIG. 3. The thermal evolution of the C_iO_i defect for the Sn_L and Sn_H samples.

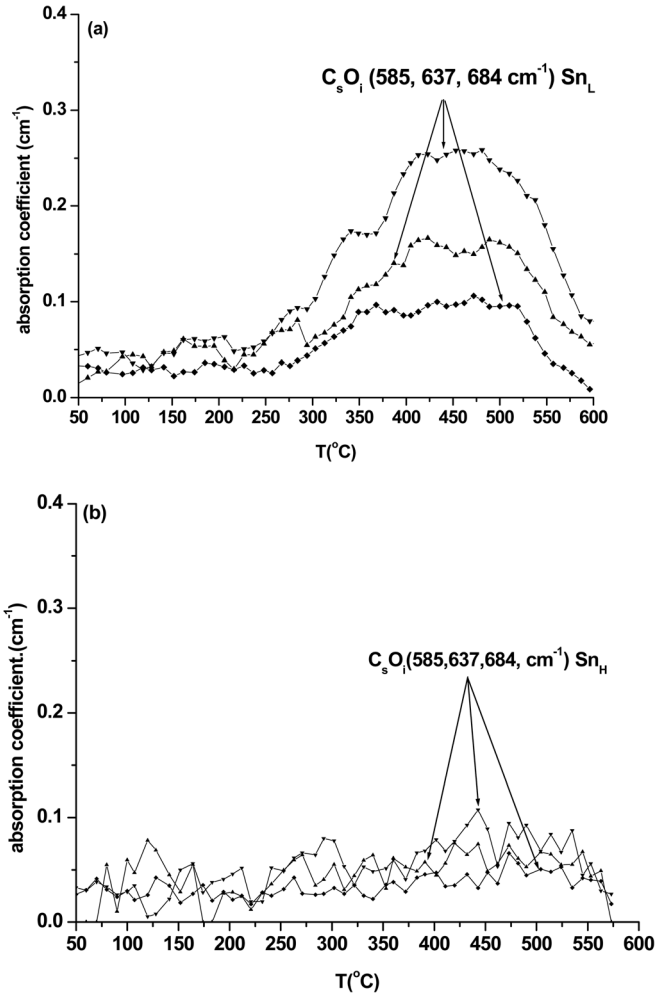

FIG. 4. The thermal evolution of the C_sO_i (585-, 637-, 685-cm^{-1}) defects for the Sn_L (a), and Sn_H (b) samples.

where the repulsion is reduced) and the attractive interaction of the SnC_s (Sn and C_s at nearest-neighbor positions where their binding is maximized).

Figure 6 corresponds to Fig. 3, except for the C_iC_s/C_iO_i defects, which contribute to the $546\,cm^{-1}$ band. Figure 7 corresponds to Fig. 3 except for the $C_iO_i(Si_I)$ defects. It is evident from Figs. 3, 4, 6, and 7, as well as from the results cited in Table I, that the production of the carbon-related defects [C_iO_i, C_sO_i, C_iC_s, and $C_iO_i(Si_I)$] is suppressed in the highly Sn-doped sample. Notably, photoluminescence (PL) studies have shown a reduction of the carbon-related defects C_iO_i and C_iC_s in 61-MeV proton-irradiated Fz-Si.[50,55] It is well known that Sn atoms interact with C_i atoms to form SnC_i complexes, and certain IR bands at 873.5, 1025, and $6875\,cm^{-1}$ have been correlated with this center.[7] We note that the defect anneals out just above room temperature.[7] Thus, during the irradiations at 80 °C the defect is expected to form and dissociate immediately. This is the reason we have not detected the corresponding signals from the defect. As we mentioned above, the results show a small but clear effect on the production of interstitial related defects in agreement with PL data, but in contrast to previous reports.[5,6,50,55] Actually, the formation of the C-related centers C_iO_i, C_iC_s, and $C_iO_i(Si_I)$ is slightly reduced between the

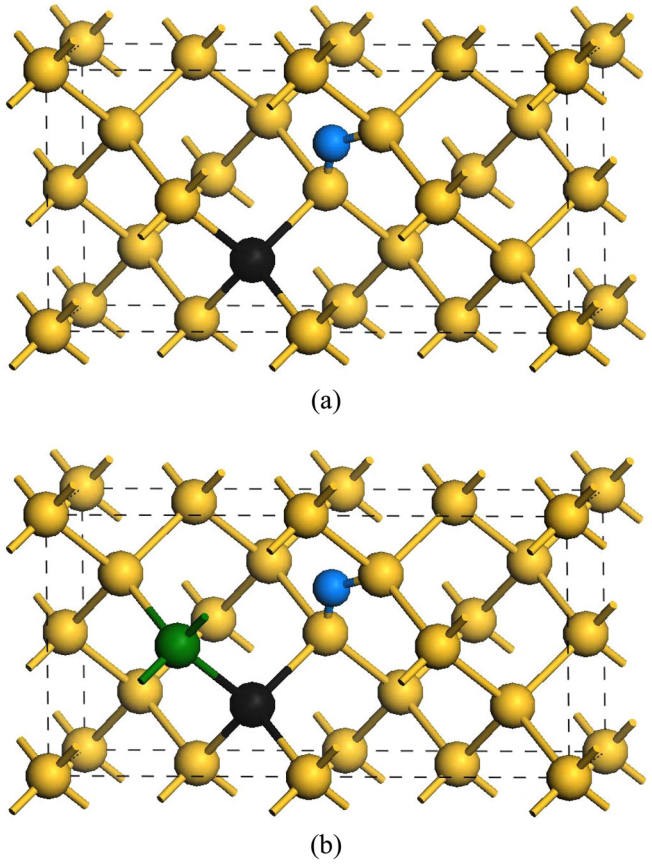

FIG. 5. (Color online) Schematic representations of the most bound (a) C_sO_i pair, and (b) SnC_sO_i cluster in Si. Grey (yellow) and dark grey (green) spheres represent the Si and Sn atoms respectively. Small (blue) and black spheres represent O_i and C_s, respectively.

Sn_L and Sn_H samples. A possible explanation can be the following: a fraction of the C_i impurities is trapped by Sn in the course of irradiation. These SnC_i defects are unstable in the temperature of irradiation and, therefore, because of their dissociation, the interstitial carbon atoms can be immediately released. Reasonably, parts of these C_i return to substitutional sites forming C_s and, therefore, the total amount of

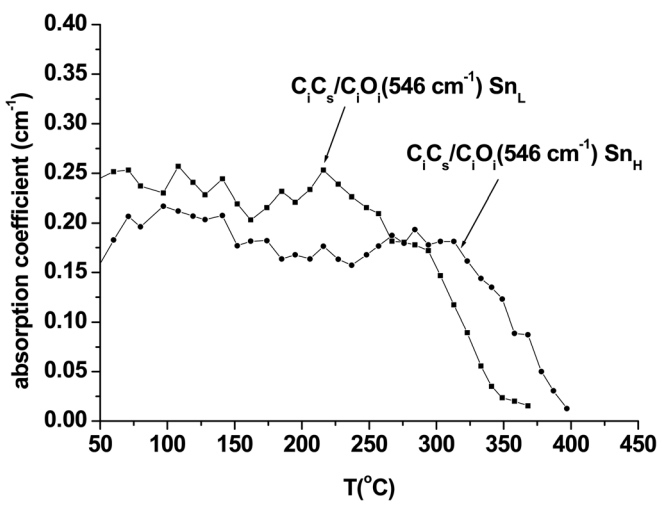

FIG. 6. The thermal evolution of the 546 cm^{-1} band of the C_iO_i/C_iC_s defects for the Sn_L and Sn_H samples.

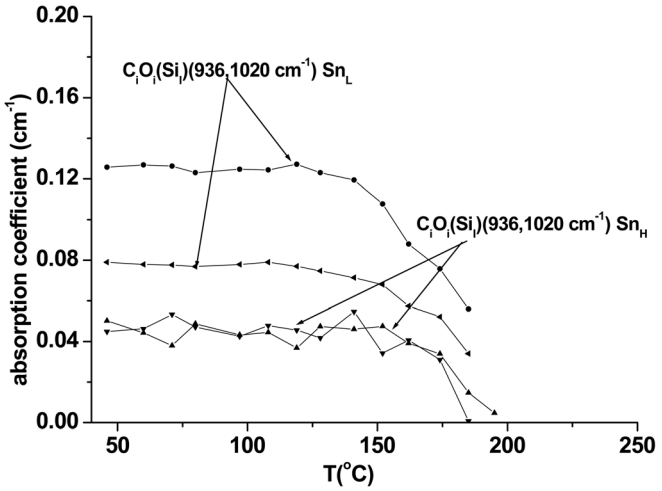

FIG. 7. The thermal evolution of the $C_iO_i(Si_I)$ defects for the Sn_L and Sn_H samples.

carbon atoms that participate in the formation of the C_iO_i, C_iC_s, and $C_iO_i(Si_I)$ complexes is expected to be reduced in the Sn-doped material. Within the framework of this argument, the higher the Sn-content in Si, the more we expect the reduction in the formation of the centers. This is reflected in the present spectra by the reduction of the amplitudes of the above C-related bands in the Sn_H sample. Notably, an alternative explanation of the lower formation of C_i-related centers in Sn-doped material exists.[56] It is established that C_iO_i and C_iC_s pairs form upon the capture of diffusing C_i by O_i and C_s at around room temperature. The C_i defects appear by means of a kick-out mechanism (i.e., the displacement of C_s) in the presence of diffusing self-interstitials. If a self-interstitial or C_i effectively decrease the diffusivity, one might expect a decrease in the formation of C_i-related centers. Sn atoms may act as "scattering" centers for diffusing C_i or Si_I, and their diffusivity may in turn decrease by increasing their "effective diffusion length."[56]

Notably, Backlund and Estreicher[46] used DFT to calculate that the C_iO_i pair (binding energy -1.64 eV) is more bound compared to $C_iO_i(Si_I)$ (binding energy -1.50 eV). This will effectively imply that when a pre-existing C_iO_i pair encounters a Si_I it will repel it. The formation of the $C_iO_i(Si_I)$ cluster can, however, be possible under conditions of a self-interstitial supersaturation, as is the case of the high-radiation dose.[2] As mentioned above, an increased Sn content in Si reduces the formation $C_iO_i(Si_I)$. Intuitively, one might consider that the Si lattice is not able to accommodate Sn atoms next to Si_I, as there will be two oversized defects in the lattice. Interestingly, DFT calculations reveal that Sn substitutional atoms attract with Si_I but with only a small binding energy (-0.05 eV) at nearest-neighbor configurations. If the Sn atom is placed further away at a second-nearest-neighbor site, with respect to Si_I, the pair is relatively (to the nearest-neighbor configuration) more bound, but again by only a small energy (-0.13 eV). These calculations, therefore, are consistent with the viewpoint that Sn will effectively not associate with Si_I especially at higher temperatures and that the trapping efficiency of Sn is limited. This implies that there will be insignificant interaction of Sn with Si_I containing clusters such as

$C_iO_i(Si_I)$. For completeness, the same DFT method was used to assess the binding of C_s with Si_I. The nearest-neighbor and second-nearest-neighbor binding energies of the C_sSi_I pair are -1.46 eV and -0.23 eV, respectively. These results indicate that the C_s atoms will strongly attract Si_I, whereas for Sn the attraction will be very limited. In effect, it is expected that the C_iO_i, and $C_iO_i(Si_I)$ clusters will be less bound in the presence of Sn in Sn-doped Si compared to undoped Si and this will be predominantly because of the repulsion of Sn with O_i (1.26 eV).[54]

The experimental results (Figs. 3, 4, 6, and 7) also demonstrate that the thermal stability of C_iO_i, C_iC_s, and $C_iO_i(Si_I)$ clusters is slightly enhanced. This may be the result of strains induced in the Si lattice by the larger substitutional Sn atoms. The activation energy that characterizes the annealing of the C-related defects may be larger in the presence of Sn, which is reflected in our spectra by the delay in their disappearance. That is, they seem to begin to migrate or dissociate at higher temperatures.

Comparing with Ge-doped material, some similarities and differences can be observed in the behavior of the radiation-induced defects. First, the production of oxygen-vacancy defects is increased in Ge-doped Si although in Sn-doped Si is reduced.[31] The conversion of VO to VO_2 is reduced with the increase of the concentration of the isovalent dopant both for germanium and Sn-doped material.[33] A small delay is observed in the growth of the VO_2 defect in Sn-doped Si in comparison with the Ge-doped Si, where an opposite trend was recently reported.[29] Concerning the C-related centers, the Sn doping reduce their production. The same trend is determined in Ge-doped material for high Ge concentrations.[32] The thermal stability of the C-related defects is slightly enhanced because of Sn doping. In the case of Ge doping, this effect is practically unimportant with the thermal stability of the C_iO_i pair only slightly decreasing and that of the C_iC_s pair to be slightly increasing.[29]

VO and V_2 defects produced by irradiation are important recombination centers in Si. Both of them introduce electrical levels in the gap and their presence is critical for lifetime control of Si-based electronic devices.[57,58] Concerning VO defect, our results indicate that Sn doping, at a concentration of $\sim 10^{19}$ cm^{-3}, results in a substantial reduction of the VO concentration, which has an important beneficial effect regarding radiation hardness of the material. The usefulness in practical applications such as radiation defects is obvious. Additionally, Sn doping reduces the formation of carbon-related defects increasing slightly their thermal stability. The present results verify previous reports that Sn doping in Si is an important tool in studying radiation defects and their properties.[50]

IV. SUMMARY

Although the importance of the interaction of isovalent impurities with point defects in group-IV semiconductors was discussed in previous studies, the present investigation is the first to systematically address these issues in Sn-doped Cz-Si from both FTIR and DFT perspectives.[50,59–66] Here we focus on the impact of Sn-doping on the oxygen and carbon defects in Cz-Si. The FTIR results determine the thermal stability of the defect clusters, whereas the DFT results provide evidence on the binding energies (i.e., if the clusters will form and what will be their relative concentration).

The experimental results verify previous reports that the production of VO defect is largely suppressed in Sn-doped Si because of the preferential capture of vacancies. The conversion of VO to VO_2 is largely reduced because of the formation of SnVO defects. The growth of the VO_2 defect in the spectra shows a small delay in the highly Sn-doped material. Additionally, experimental evidence is provided that Sn doping suppresses the formation of the carbon-related [C_iO_i, C_iC_s, $C_iO_i(Si_I)$] defects, although it slightly enhances their thermal stability. Their decreased formation can be ascribed to the tendency of Sn to pair momentarily with carbon during irradiation, leading to a decreased availability of carbon impurities to form C-related defects. Regarding the enhancement of their thermal stability, an explanation may be envisaged by taking into account the strains induced in the Si lattice by the larger substitutional Sn impurities. Any difference between the impact of Sn and Ge on the stability of C-related defects may also be connected with the differences between Sn and Ge isovalent impurities regarding their interactions with intrinsic defect and carbon atoms.

From an atomistic simulation perspective the two basic interactions are the attraction of the Sn to the vacancies (or small substitutional defects such as C_s) and its strong repulsion to O_i interstitial defects. Therefore, the presence of Sn can directly increase the binding energy of defects such as VO, whereas it will not directly associate with others such as C_iO_i. In any case, Sn can indirectly influence the formation of clusters, as it will associate with point defects influencing their concentration. The reason for investigating samples with two concentrations of Sn, one below and one above 10^{18} cm^{-3}, is that it will have a significant effect on the defect processes. For example, the experimental results determine that the formation of VO defect is largely suppressed in Sn-rich Si because of the capture of V by the Sn atoms. This can lead to the suppression of the conversion of VO to VO_2 because of the formation of SnVO clusters. Future studies need to systematically assess the impact of Sn content on the formation and thermal stability of clusters and to discover the optimum Sn-doping strategy that most efficiently reduces the concentration of technologically harmful clusters.

ACKNOWLEDGMENTS

Computing resources were provided by the HPC facility of Imperial College London where A. Chroneos is a Visiting Academic.

[1] P. Pichler, in *Intrinsic Point Defects, Impurities and Their Diffusion in Silicon*, edited by S. Selberherr (Springer Verlag, Wien, 2004).
[2] G. Davies and R. C. Newman, in *Handbook in Semiconductors*, edited by S. Mahajan, (Elsevier, Amsterdam, 1994), Vol. 3, pp. 1557–1635.
[3] G. D. Watkins, Phys. Rev. B **12**, 4383 (1975).
[4] B. G. Svensson, J. Svensson, G. Davies, and J. W. Corbett, Appl. Phys. Lett. **51**, 2257 (1987).
[5] A. Brelot, IEEE Trans. Nucl. Sci. **19**, 220 (1992).

[6]A. Brelot, in *Radiation Damage and Defects in Semiconductors*, edited by J. E. Whitehouse (Institute of Physics, London, 1973), Conference Series No. 16, p. 191.
[7]E. V. Lavrov, M. Fanciulli, M. Kaukonen, R. Jones, and P. R. Briddon, Phys. Rev. B **64**, 125212 (2001).
[8]L. T. Canham, M. R. Dyball, and K. G. Barraclough, Mater. Sci. Eng., B **4**, 95 (1989).
[9]G. D. Watkins, in *Deep Centers in Semiconductors: A State-of-the-Art Approach*, edited by S. T. Pantelides (Gordon and Breach, New York, 1986), p. 147.
[10]H. Höhler, N. Atodiresei, K. Schroeder, R. Zeller, and P. H. Dederichs, Phys. Rev. B **71**, 035212 (2005).
[11]A. Nylandsted Larsen, J. J. Goubet, P. Mejlholm, J. Sherman Christensen, M. Fanciulli, H. P. Gunnlaugsson, G. Weyer, J. Wulff Petersen, A. Resende, M. Kaukonen, R. Jones, S. Öberg, P. R. Briddon, B. G. Svensson, J. L. Lindström, and S. Dannefaer, Phys. Rev. B **62**, 4535 (2000).
[12]J. L. Lindstrom and B. G. Svensson, Mater. Res. Soc. Symp. Proc. **59**, 45 (1986).
[13]R. C. Newman, *Infrared Studies of Crystal Defects* (Taylor & Francis, London, 1973).
[14]J. W. Corbett, G. D. Watkins, and R. S. Mc Donald, Phys. Rev. **135**, A1381 (1964).
[15]C. A. Londos, N. V. Sarlis, L. G. Fytros, and K. Papastergiou, Phys. Rev. B **53**, 6900 (1996).
[16]M. Fanciulli and J. R. Byberg, Phys. Rev. B **61**, 2657 (2000).
[17]M. Kaukonen, R. Jones, S. Öberg, and P. R. Briddon, Nucl. Instrum. Methods Phys. Res. B **186**, 24 (2002).
[18]L. I. Khirunenco, O. A. Koobzar, Y. V. Pomozov, M. G. Sosnin, N. A. Tripachko, V. P. Markevich, L. I. Murin, and A. R. Peaker, Phys. Status Solidi C **0**, 694 (2003).
[19]J. M. Trombetta and G. D. Watkins, Appl. Phys. Lett. **51**, 1103 (1987).
[20]B. G. Svensson and J. L. Lindström, Phys. Status Solidi A **95**, 537 (1986).
[21]C. A. Londos, Jpn. J. Appl. Phys., Part 1 **27**, 2089 (1988).
[22]C. A. Londos, Semicond. Sci. Technol. **5**, 645 (1990).
[23]C. A. Londos, Phys. Rev. B **35**, 6295 (1987).
[24]R. C. Newman and A. R. Bean, Radiat. Eff. **8**, 189 (1971).
[25]E. V. Lavrov, L. Hoffmann, and B. B. Nielsen, Phys. Rev. B **60**, 8081 (1999).
[26]C. A. Londos, M. S. Potsidi, and E. Stakakis, Physica B **340–342**, 551 (2003).
[27]C. A. Londos, G. D. Antonaras, M. S. Potsidi, D. N. Aliprantis, and A. Misiuk, J. Mater. Sci.: Mater. Electron. **18**, 721 (2007).
[28]C. A. Londos, G. D. Antonaras, M. S. Potsidi, and A. Andrianakis, Physica B **376–377**, 165 (2006).
[29]C. A. Londos, A. Andrianakis, E. N. Sgourou, V. Emtsev, and H. Ohyama, J. Appl. Phys. **107**, 093520 (2010).
[30]C. A. Londos, A. Andrianakis, V. Emtsev, G. A. Oganesyan, and H. Ohyama, Mater. Sci. Eng., B **154**, 133 (2008).
[31]C. A. Londos, A. Andrianakis, V. Emtsev, and H. Ohyama, Semicond. Sci. Technol. **24**, 075002 (2009).
[32]C. A. Londos, A. Andrianakis, V. Emtsev, G. A. Oganesyan, and H. Ohyama, Physica B **404**, 4693 (2009).
[33]C. A. Londos, A. Andrianakis, E. N. Sgourou, V. Emtsev, and H. Ohyama, J. Appl. Phys. **109**, 033508 (2011).
[34]A. Baghdadi, W. M. Bullis, M. C. Choarkin, Y. Li, R. I. Scace, R. W. Series, P. Stallhofer, and M. Watanabe, J. Electrochem. Soc. **136**, 2015 (1989).
[35]J. L. Regolini, J. P. Stroquert, C. Ganter, and P. Siffert, J. Electrochem. Soc. **133**, 2165 (1986).
[36]M. D. Segall, P. J. D. Lindan, M. J. Probert, C. J. Pickard, P. J. Hasnip, S. J. Clark, and M. C. Payne, J. Phys.: Condens. Matter **14**, 2717 (2002).
[37]J. Perdew, K. Burke, and M. Ernzerhof, Phys. Rev. Lett. **77**, 3865 (1996).
[38]D. Vanderbilt, Phys. Rev. B **41**, 7892 (1990).
[39]H. J. Monkhorst and J. D. Pack, Phys. Rev. B **13**, 5188 (1976).
[40]D. Caliste, P. Pochet, T. Deutsch, and F. Lançon, Phys. Rev. B **75**, 125203 (2007).
[41]A. Chroneos, H. Bracht, R. W. Grimes, and B. P. Uberuaga, Appl. Phys. Lett. **92**, 172103 (2008).
[42]A. Chroneos, H. Bracht, C. Jiang, B. P. Uberuaga, and R. W. Grimes, Phys. Rev. B **78**, 195201 (2008).
[43]M. I. J. Probert and M. C. Payne, Phys. Rev. B **67**, 075204 (2003).
[44]A. Chroneos, Phys. Status Solidi B **244**, 3206 (2007).
[45]A. Chroneos, C. Jiang, R. W. Grimes, U. Schwingenschlögl, and H. Bracht, Appl. Phys. Lett. **94**, 252104 (2009).
[46]D. J. Backlund and S. K. Estreicher, Phys. Rev. B **77**, 205205 (2008).
[47]C. A. Londos, L. G. Fytros, and G. J. Georgiou, Defect Diffus. Forum **171–172**, 1 (1999).
[48]N. Inoue, H. Ohyama, Y. Goto, and T. Sugiyama, Physica B **401–402**, 477 (2007).
[49]V. P. Markevich, A. R. Peaker, B. Hamilton, V. V. Litvinov, Yu. M. Pokotilo, S. B. Lastovskii, J. Coutinho, A. Carvalho, M. J. Rayson, and P. R. Briddon, J. Appl. Phys. **109**, 083705 (2011).
[50]C. Claeys, E. Simoen, V. P. Neimash, A. Kraitchinskii, M. Kras'ko, O. Puzenko, A. Blondeel, and P. Clauws, J. Electrochem. Soc. **148**, G738 (2001).
[51]V. D. Ahmetov and V. V. Bolotov, Radiat. Eff. **52**, 149 (1980).
[52]Y. H. Lee, Appl. Phys. Lett. **73**, 1119 (1998).
[53]L. I. Khirunenko, O. O. Koibzar, Yu. V. Pomozov, M. G. Sosnin, and M. O. Tripachko Physica B **340–342**, 541 (2003).
[54]A. Chroneos and C. A. Londos, J. Appl. Phys. **107**, 093518 (2010).
[55]E. Simoen, C. Clays, V. Privitera, S. Coffa, M. Kokkoris, E. Kossionides, G. Fanourakis, A. Nylandsted Larsen, and P. Claws, Nucl. Instrum. Methods Phys. Res. B **186**, 19 (2002).
[56]A. Nylandsted Larsen, A. Bro Hansen, D. Reitze, J. J. Goubel, J. Fage-Pedersen, and A. Mesli, Phys. Rev. B **64**, 233202 (2001).
[57]S. D. Brotherton and P. Bradley, J. Appl. Phys. **53**, 5720 (1982).
[58]R. Siemieniec, F. J. Niedernostheide, H. J. Schulze, W. Südkamp, U. Kellner- Wesdenansen and J. Lutz, J. Electrochem. Soc. **153**, G108 (2006).
[59]A. Chroneos, J. Appl. Phys. **107**, 076102 (2010).
[60]A. B. Gerasimov, M. K. Gototishvili, and B. M. Konovanenko, Semiconductors **20**, 1243 (1986).
[61]A. Chroneos, H. Bracht, R. W. Grimes, and B. P. Uberuaga, Mater. Sci. Eng. B **154–155**, 72 (2008).
[62]A. Chroneos, J. Appl. Phys. **105**, 056101 (2009).
[63]A. Chroneos, R. W. Grimes, and H. Bracht, J. Appl. Phys. **105**, 016102 (2009).
[64]A. Chroneos, C. A. Londos, and H. Bracht, Mater. Sci. Eng. B **176**, 453 (2011).
[65]A. Chroneos, Semicond. Sci. Technol. **26**, 095017 (2011).
[66]C. A. Londos, E. N. Sgourou, A. Chroneos, and V. V. Emtsev, Semicond. Sci. Technol. **26**, 105024 (2011).